

# Analysis of stepper motor dynamics using numerical methods

Radosław Kępiński, Jan Awrejcewicz, Jakub Gajek

*Abstract:* Hybrid stepper motors, because of non-linear nature of the governing ordinary differential equations as well as the non-continuous character of the excitation voltage, exhibit a behaviour interesting from a point of view of system dynamics. In this paper, dynamical properties of such electrical machines is studied with a help of mathematical modelling and numerical integration methods. By using experimental data, parameters of a real object are identified and used to simulate its response under a number of circumstances. To get a grasp of the dynamical phenomena occurring during motor's operation, standard methods for analysis of system dynamics (such as Poincaré sections and bifurcation diagrams) are applied. As the simulation results show good agreement with the experimental observations, conclusions can be drawn concerning currently used methods of controlling hybrid stepper motors and some of their disadvantages.

## 1. Introduction

### 1.1. Scope of the research

In the following investigations we analyse the dynamics of a system consisting of a hybrid stepper motor loaded with a rotating cylindrical mass. Such synchronous machines are commonly used in a number of industrial and household mechatronic devices such as positioning systems, scanners, printers, digital cameras, optical drives, etc.

Their main advantage is that they can be used in design of very compact and simple positioning systems using the open-loop approach, i.e. there is no need for a position feedback. This is especially advantageous when designing small or miniature devices. However, those features come with a drawback of having to incorporate an appropriate control system (driver), that is relatively more sophisticated than, for instance, in the case of DC motors. This is because a number of methods increasing the system performance are commonly used, such as voltage chopping and micro-stepping [1, 10].

It is known that for certain rotational speeds this type of motor can exhibit undesired behaviour, associated with its synchronous nature. For example rotor stalling may occur when either the stepping frequency is too high or close to the resonance regions or there is a sudden peak in the load torque. Because the ODEs governing such electrical motors

are of non-linear nature, analysis of similar problems have drawn the attention of some researchers [3, 6, 12].

Using approaches common in dynamical analysis, we try to understand the behaviour of such systems on the basis of numerical simulations, as well as experimental set-up measuring phase currents during the motor's operation. Such analysis can prove crucial in efforts to improve positioning accuracy and system performance by incorporating novel control methods such as those described in [2, 4, 7, 9].

## 1.2. Physical system

The physical system being considered in this research consists of the following components:

- hybrid, two phase, bipolar stepper motor,
- stepper motor driver,
- programmable logic controller (PLC),
- 36V DC power supply unit,
- incremental rotary encoder.

The overview of the system is presented in Fig. 1. It can be seen that the velocity and position control is done by the PLC which serves as indexer and passes appropriate pulse signal to the driver. This device generates the required voltages on the motor's windings using the electrical power from the dedicated power supply. In this system a position feedback using a rotary encoder has been introduced to allow for measuring the system response. This allows detecting when the set and actual angular velocities of the rotor start to drift away from each other, resulting in a loss of synchronism. Mechanical part of the system can be

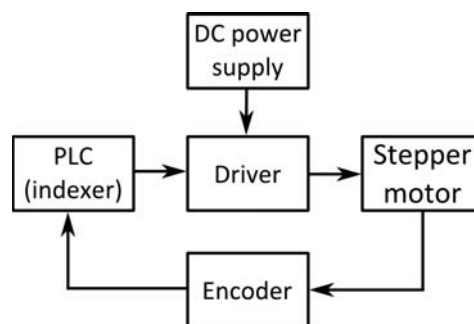


**Figure 1.** Overview of the considered electro-mechanical system.

seen in the photo presented in Fig. 2. It consists of a shaft and cylindrical mass supported on a ball bearing coupled with the motor using Oldham coupler.

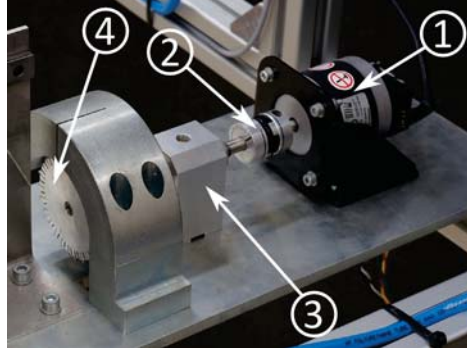


**Figure 2.** Mechanical system: stepper motor (1), Oldham coupler (2), ball bearing support (3), rotating mass (4).

## 2. Mathematical model

In what follows, we assume the physical model of the considered system shown in Fig. 3. We model two windings with their respective resistances ( $R$ ) and inductances ( $L$ ), as well as voltage sources  $V_A$  and  $V_B$ . The rotor of a hybrid motor consists of alternately placed permanent magnet poles with equally spaced grooves around its circumference, that ensure variable reluctance of distinct rotor positions.

According to a number of authors [5, 8, 11] in the case of a two phase stepper motor, one can write four ordinary differential equations. Two of them are derived from the 2nd Kirchhoff Law and the remaining two are Newton's 2nd Law of Motion. In the case of a system considered in this paper, they have been cast into the following form:

$$\begin{aligned}
 L \frac{dI_A}{dt} &= V_A - RI_A + K_m \omega \sin(N_r \varphi), \\
 L \frac{dI_B}{dt} &= V_B - RI_B - K_m \omega \cos(N_r \varphi), \\
 J \frac{d\omega}{dt} &= -K_m I_A \sin(N_r \varphi) + K_m I_B \cos(N_r \varphi) - b\omega, \\
 \frac{d\varphi}{dt} &= \omega,
 \end{aligned} \tag{1}$$

where:  $I_A$ ,  $I_B$  are currents in both phases;  $V_A$  and  $V_A$  are voltages applied to the windings;  $R$ ,  $L$  are winding's resistance and inductance, respectively;  $K_m$  is the motor torque constant,  $b$  is viscous friction coefficient,  $N_r$  is the number of rotor teeth,  $J$  is rotor's moment of inertia,  $\omega$  is the rotor speed and  $\varphi$  is its angular position.

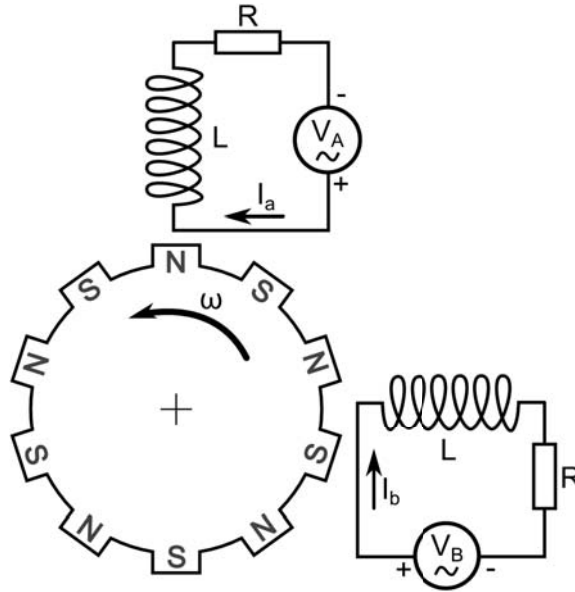


**Figure 3.** Schematic of a two phase hybrid stepper motor.

In the proposed mathematical model we assume the load on the motor comes only from the inertia of the cylindrical mass and the linear friction (coming mainly from bearings on which the device is supported).

Modelling the excitation voltages  $V_A$  and  $V_B$  as they appear in a real stepper driver is however a little problematic. First of all, they are non-continuous, because of the stepping nature of the system, which requires appropriate approach to the numerical integration. More importantly, because it is common to use voltage chopping to increase the performance of the system,  $V_A$  and  $V_B$  are not only time dependant but also depend on  $I_A$  and  $I_B$  respectively.

### 3. Experimental investigations

To perform identification of system parameters as well as to confirm the behaviour of the system observed during numerical simulations, there is a need to proceed with a suitable experiment. Owing to (1), we know that the state of the system is fully defined by a following vector:  $[I_A, I_B, \varphi, \omega]^T$ . Therefore in addition to a rotary encoder, a measurement circuit for phase currents is necessary.

### 3.1. Experimental set-up

In the described experiment we use a shunt resistor current sensing method. In this approach a shunt resistor ( $R_s$ ) is introduced into the phase circuits. Because its resistance is very low comparing to the windings resistance  $R$  it does not introduce any disturbance into the motor's operation. Voltage drop on the shunt resistor allows to calculate the phase current value using the Ohm's Law.

To get reliable results an amplification circuit is necessary. In this application two bi-directional shunt current sensors with the amplification rate of 50 were used. The schematic of the measurement set up is presented in Fig. 4.

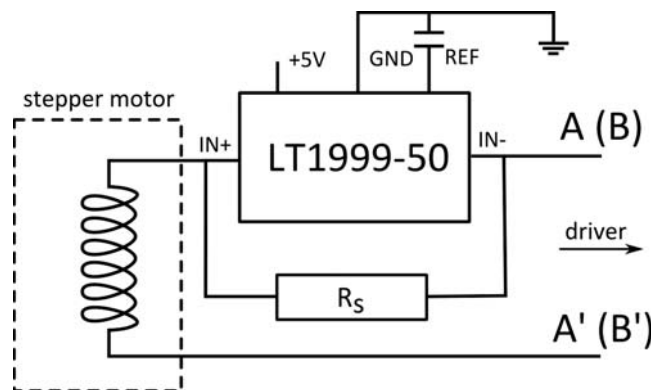


Figure 4. Phase current measurement circuit.

### 3.2. Methodology and experimental results

In the experiment the excitation frequency  $f$  was gradually increased from 30 Hz up to 20 kHz. The excitation frequency regulates how many times step counter is incremented in a unit of time. The resulting voltages from the current sensors were passed to two channels of a digital oscilloscope. As a result XY plots have been made where on X axis we put current in phase A and on Y axis current in phase B. During the measurements, the motor driver was set to 1:8 micro-stepping. The results of those investigations have been gathered in Table 1.

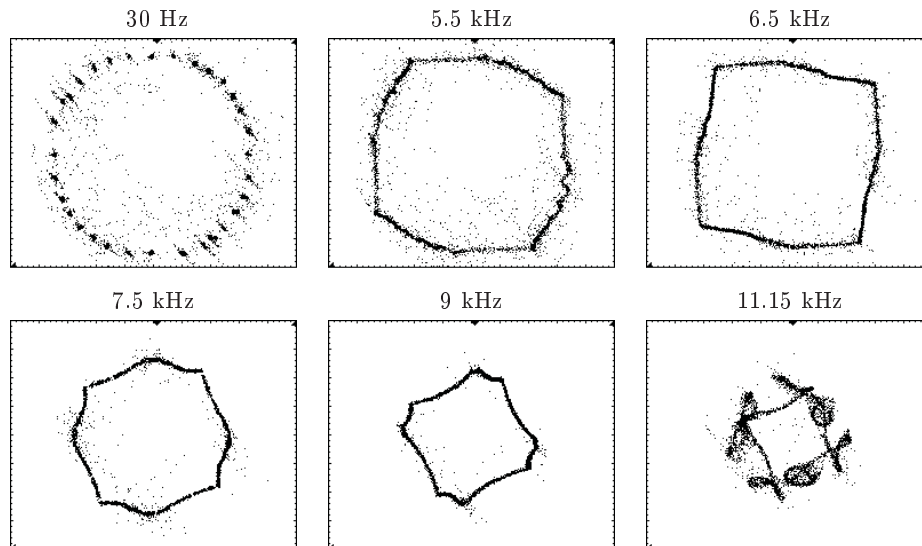
Those results allow to observe change in the trajectory on  $I_A - I_B$  plane, associated with the increase of the excitation frequency. For frequencies below 2.5 kHz distinctive points are visible that are associated with each micro-step at which the rotor becomes stationary for a short while. For this interval the curve is clearly of a circular shape. However, further increase of the parameter  $f$  yields gradual change of shape of the curve. At 5.5 kHz the trajectory resembles a slightly distorted square.

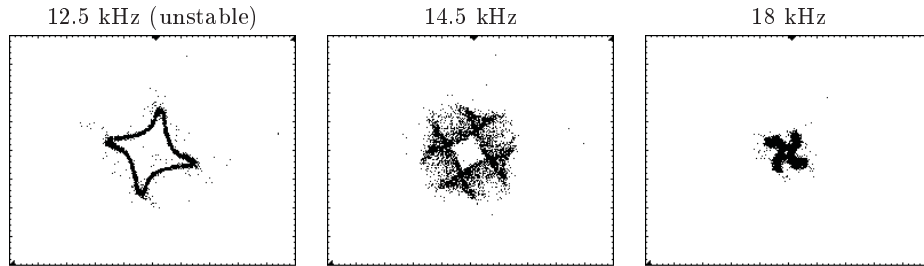
Exceeding 6 kHz results in gradual decrease of the inner area limited by the trajectory curve. It is associated with the fact that the motor's windings can no longer be fully energized. For the interval from 6 kHz to around 11 kHz we observe further decrease of the inner area, as well as a change of shape. At 11 kHz a sudden change of the trajectory shape occurs and the motor stalls. We can observe that the trajectory curve starts to intersect itself in several points. This instability phenomena takes place for the interval from 11 kHz up to 11.5 kHz.

For 11.5 up to 13.8 kHz we once again have stable operation of the system, followed by a wide instability region ending around 16.5 kHz. This region is followed by the stable operation of the motor for the interval from 16.5 to 19 kHz, while the inner area limited by the trajectory shrinks even further. At this point the motor pull-out torque is significantly reduced, and even a small peak of the load torque can lead to the loss of synchronous velocity of the rotor. For the frequencies close to the 20kHz the system in general behaved in an unstable manner. Frequencies past the 20 kHz point were not tested.

The above investigations yield results similar to [3], but quantitatively not in agreement due to the difference in stepper motor type and size. However, we can observe that when the trajectory on the  $I_A - I_B$  plane starts to intersect with itself we deal with the instability region.

**Table 1.** Results of the phase current measurements.





#### 4. Numerical analysis

To perform in-depth analysis of the dynamical properties in the described system, numerical integration methods prove to be crucial. As previously mentioned in section 2, modelling stepper motor driver is quite complex. In the following investigations we are neglecting the fact that a voltage chopper is used in a physical system. The physical parameters of the system are presented in Table 2.

Parameter	Value	Unit
$R$	5	$\Omega$
$L$	$8.6 \times 10^{-3}$	H
$b$	$6 \times 10^{-3}$	$\text{N} \cdot \text{m} \cdot \text{s}/\text{rad}$
$K_m$	0.55	$\text{N} \cdot \text{m}/\text{A}$
$V$	36	V
$J$	$179 \times 10^{-5}$	$\text{kg} \cdot \text{m}^2$
$N_r$	50	-

**Table 2.** System parameters.

Three excitation functions have been used in numerical simulation: full-stepping, half-stepping and sine wave (Fig. 5). The last of those approaches simulates micro-stepping method - when using small micro-steps (i.e. 1:8 or smaller) the excitation function can be approximated by a sine wave. The benefit of such simplification is that we do not have discontinuities in the  $V(t)$  functions, which results in much shorter simulation times.

Bifurcation diagrams (Figs. 6-11 b) were used to illustrate the dynamics of the system under respective excitation methods. The control parameter is excitation frequency  $\Psi$  and on the vertical axis we have one of phase currents (in this case  $I_A$ ). In every case  $\Psi = 2\pi\text{rad}/\text{s}$  corresponds to exactly four full steps, i.e. one full control sequence of the motor driver (as illustrated in Fig. 5).

The initial conditions are zero at the left hand side of the bifurcation diagrams, but as

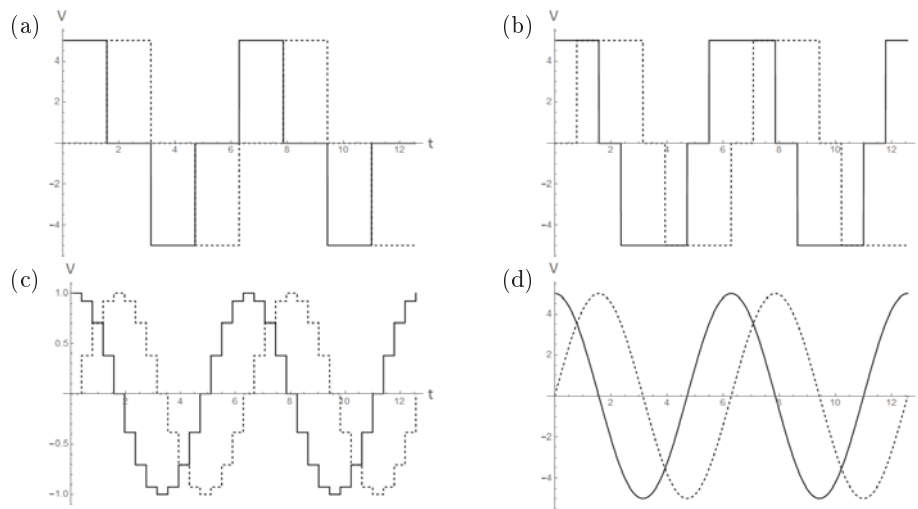


**Figure 5.** Excitation functions used in numeric simulations: (a) full-step, (b) half-step, (c) micro-step (1:8), (d) sine wave.

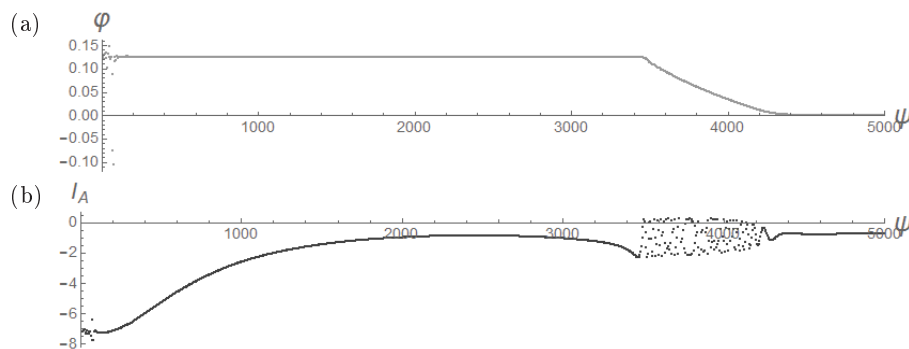


**Figure 6.** Travelled distance (a) and bifurcation diagram (b) for full-step drive with high acceleration.

we increase the value of the control parameter, we keep the end values from the previous simulation. This allows for simulating a gradually ramping up speed of the motor.

There are two bifurcation diagrams for each excitation method. The former illustrates ramping up with a higher and the latter with a lower acceleration. As can be clearly seen it has a large impact on the results. When speeding up the motor slowly we encounter instability regions associated with resonance that manifest themselves in the diagrams. This is most apparent in case of full-stepping and sine wave driver. Moreover, above the bifurcation diagrams there are plots of the distance travelled by the rotor  $\varphi$  for each of the control



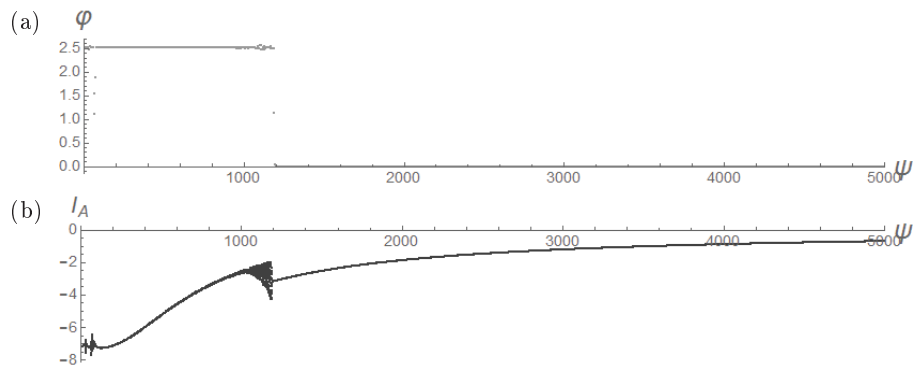


**Figure 7.** Travelled distance (a) and bifurcation diagram (b) for full-step drive with low acceleration.

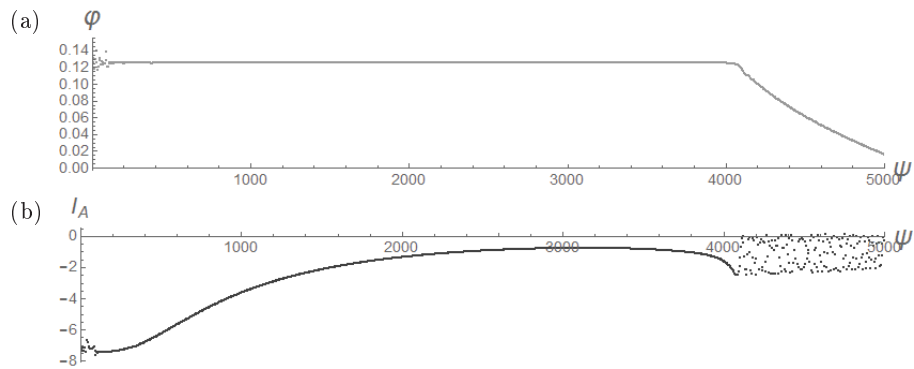


**Figure 8.** Travelled distance (a) and bifurcation diagram (b) for half-step drive with high acceleration.

parameter values. If there are no missed steps, the value is constant. When there is loss of synchronism, the motor starts to skip steps and the value tends to zero.

According to the simulation results, the highest rotational speed can be obtained with a half-step approach. There is a resonance region between 1200 and 1600  $rad/s$  that has impact on the behaviour of the system, when the acceleration speed is low, especially when the driver is in full-step mode. In general, there are two instability regions, indicated by non-periodic trajectory, which confirms the conclusions drawn from the previously described experiment.

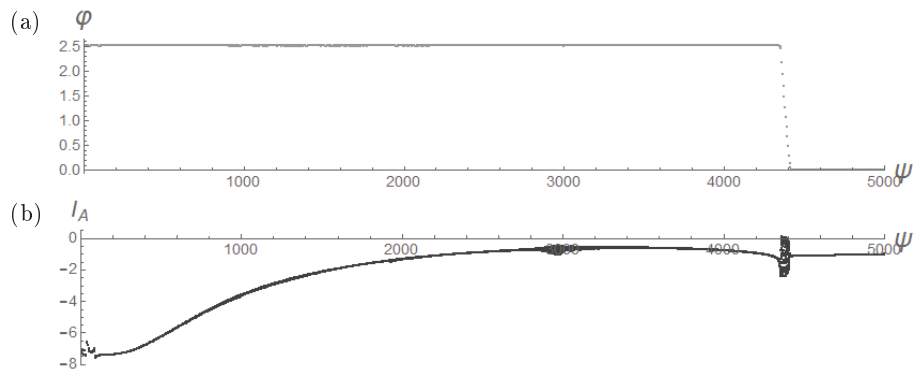


**Figure 9.** Travelled distance (a) and bifurcation diagram (b) for half-step drive with low acceleration.

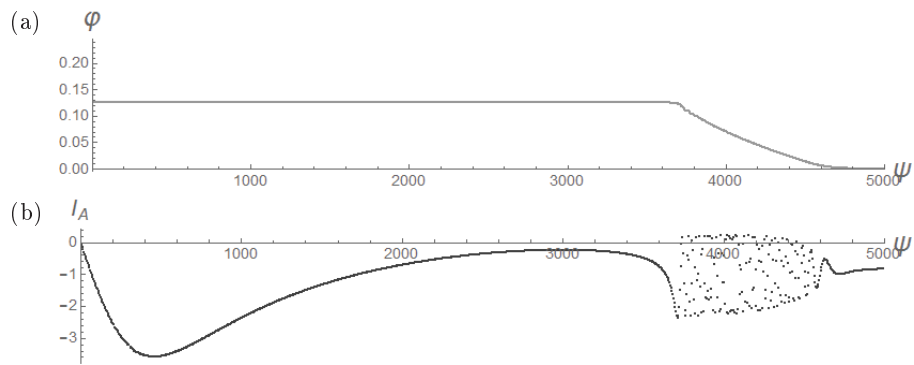


**Figure 10.** Travelled distance (a) and bifurcation diagram (b) for micro-step (sine wave excitation) drive with high acceleration.

### 5. Concluding remarks

The carried out experiment allows to study system behaviour in the wide range of excitation frequencies. During both the initial tests and the numerical simulation we detected instability regions that can be associated with the mid- and high frequency instability phenomena [1]. In each of the cases, the loss of synchronous velocity is correlated with a sudden qualitative change of the form the phase trajectory curve, e.g. the curve starts to intersect itself at several points.

Results obtained so far suggest that detecting instability regions can be possible using a relatively low-cost current sensors. Application of such method into the motor drivers can allow them to detect and avoid problems associated with the loss of synchronism.

Numerical simulation shows good correlation with these results. By the use of bifurcation

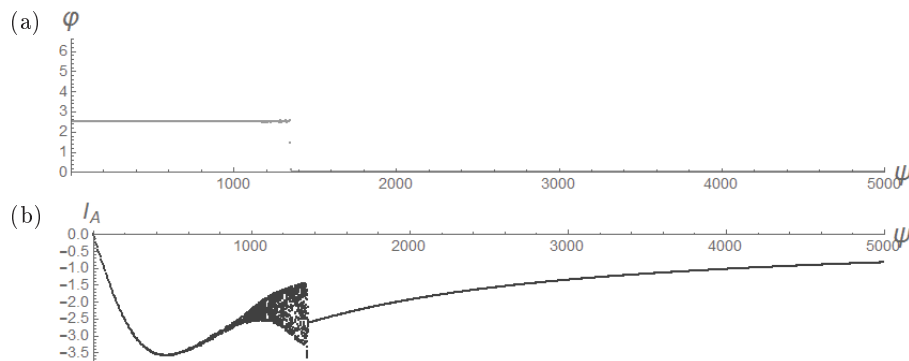


**Figure 11.** Travelled distance (a) and bifurcation diagram (b) for micro-step (sine wave excitation) drive with low acceleration.

diagrams we were able to analyse the behaviour of the system using full-step, half-step and micro-step drivers. Unstable regions of operation are clearly visible on the diagrams as non-periodic trajectories and associated travel distance plots show missed steps as the synchronous speed cannot be maintained. It has been pointed out that the acceleration rate plays a big role in the response of such systems.

The correlation between the simulation and the experiment can be further improved by modelling voltage chopper as an element of motor driver. In further research the authors hope to improve the experimental set-up by, in particular, increasing the sampling rate of the current sensors as well as acquiring the data in a raw form for future processing.

## References

- [1] ACARNLEY, P. P. *Stepping Motors: A Guide to Theory and Practice*, 4th ed. IEE Control Engineering Series. The Institution of Electrical Engineers, 2002.
- [2] ADAMS, K., AND VANREENEN, M. A low-cost stepper motor positioning system with minor closed-loop control. *The International Journal of Advanced Manufacturing Technology* 10, 3 (1995), 191–197.
- [3] BALAKRISHNAN, K., UMAMAHESWARI, B., AND LATHA, K. Identification of resonance in hybrid stepper motor through measured current dynamics in online for accurate position estimation and control. *Industrial Informatics, IEEE Transactions on* 9, 2 (2013), 1056–1063.
- [4] BANIHANI, S., AL-WIDYAN, K., AL-JARRAH, A., AND ABABNEH, M. A genetic algorithm based lookup table approach for optimal stepping sequence of open-loop stepper motor systems. *Journal of Control Theory and Applications* 11, 1 (2013), 35–41.

- [5] BODSON, M., CHIASSON, J., NOVOTNAK, R., AND REKOWSKI, R. High performance nonlinear feedback control of a permanent magnet stepper motor. In *Control Applications, 1992., First IEEE Conference on* (1992), pp. 510–515 vol.1.
- [6] CAO, L., AND SCHWARTZ, H. M. Oscillation, instability and control of stepper motors. *Nonlinear Dynamics* 18, 4 (1999), 383–404.
- [7] ELSODANY, N. M., REZEKA, S. F., AND MAHAREM, N. A. Adaptive {PID} control of a stepper motor driving a flexible rotor. *Alexandria Engineering Journal* 50, 2 (2011), 127 – 136.
- [8] KENJŌ, T. *Stepping Motors and Their Microprocessor Control*. Monographs in Electrical and Electronic Engineering. Clarendon Press, 1984.
- [9] KIM, W., SHIN, D., AND CHUNG, C. C. The lyapunov-based controller with a passive nonlinear observer to improve position tracking performance of microstepping in permanent magnet stepper motors. *Automatica* 48, 12 (2012), 3064 – 3074.
- [10] KUO, B., AND TAL, J. *Incremental Motion Control: Step motors and control systems*. Incremental Motion Control. SRL Publishing Company, 1979.
- [11] LYSHEVSKI, S. E. *Electromechanical Systems, Electric Machines and Applied Mechatronics*. Electric power engineering series. CRC Press, 2000.
- [12] RIGHETTINI, P., STRADA, R., OLDANI, A., AND GINAMMI, A. An experimental investigation on the dynamic behavior of step motor drives. *Journal of Mechanics Engineering and Automation* 2 (2012), 431–440.

Radosław Kępiński, M.Sc. (Ph.D. student): Lodz University of Technology, Department of Automation, Biomechanics and Mechatronics, 90-924 Łódź, ul. Stefanowskiego 1/15, Poland ([radoslaw.kepinski@dokt.p.lodz.pl](mailto:radoslaw.kepinski@dokt.p.lodz.pl)). The author gave a presentation of this paper during one of the conference sessions.

Jan Awrejcewicz, Professor: Lodz University of Technology, Department of Automation, Biomechanics and Mechatronics, 90-924 Łódź, ul. Stefanowskiego 1/15, Poland ([jan.awrejcewicz@p.lodz.pl](mailto:jan.awrejcewicz@p.lodz.pl)).

Jakub Gajek, M.Sc. (Ph.D. student): Lodz University of Technology, Department of Automation, Biomechanics and Mechatronics, 90-924 Łódź, ul. Stefanowskiego 1/15, Poland ([gajek.jakub@gmail.com](mailto:gajek.jakub@gmail.com)).